

# Key Oncogenic Ras Mutations Impair Limiting Proton Transfer Rates

Dénes Berta, Sascha Gehrke, Edina Rosta\*

Department of Physics and Astronomy, University College London

**KEYWORDS** *Ras GTPase, QM/MM, enhanced sampling, mechanism, proton transfer*

**ABSTRACT:** Ras-positive cancer constitutes a major challenge for medical treatment. Hot spot residues Gly12, Gly13 and Gln61 constitute the majority of oncogenic mutations which are associated with detrimental clinical prognosis. Here we present a two-step mechanism of GTP hydrolysis of the wild type Ras.GAP complex using QM/MM free energy calculations with the finite-temperature string method. We found that the deprotonation of the catalytic water takes place via the Gln61 as a transient Brønsted base. We obtained reaction profiles for key oncogenic Ras mutants G12D and G12C, reproducing the experimentally observed loss of catalytic activity, and validating our reaction mechanism.

The Ras protein isoforms are essential components of key signaling networks to promote cell proliferation and survival.<sup>1</sup> It is the most frequently mutated protein in all cancer. Ras oncogenes are involved in more than 30% of all human cancer,<sup>2–5</sup> including 98% of pancreatic cancer,<sup>6</sup> 52% of colorectal cancer<sup>7,8</sup> as well as in melanoma<sup>9–11</sup>, and lung cancer.<sup>12,13</sup> Additionally, the prognosis for Ras-positive cancer cases is significantly worse than without Ras mutations.<sup>7,11,14–16</sup> Despite more than three decades of extensive research, no effective pharmacological inhibitors of the Ras oncoproteins have reached the clinic, terming Ras proteins as 'undruggable'.<sup>17–19</sup> New therapies are therefore highly sought after.

Ras is a small GTPase, that binds GTP with very high, picomolar affinity (Figure 1).<sup>17</sup> In its GTP-bound form, Ras is active and promotes signaling for cell proliferation. To turn signaling off,<sup>20,21</sup> Ras hydrolyses GTP to GDP with the help of GTPase-activating proteins (GAPs), typically p120GAP or Ras p21.<sup>22,23</sup> GAP completes the environment around the active site (Figure 1A), it contains key conserved motifs, including an arginine finger (Figure 1B)<sup>24</sup> to enable effective catalysis. However, key oncogenic mutations render Ras catalytically inactive, and thus Ras stays in its active signaling, GTP-bound form.

There are three principal isoforms of Ras: KRas, HRas and NRas.<sup>2</sup> The differences between these are mainly related to localization and trafficking of the proteins to reach their signaling partners, while their active sites are identical. Importantly, the most frequent oncogenic mutations correspond to only three active site residues: Gly12, Gly13 and Gln61 (Figure 1C), totaling to over 97% of all Ras mutations.<sup>3</sup> Here we focus on the key oncogenic mutation site Gly12. G12D is overwhelmingly the most frequent Ras mutation, present in half of the Ras positive cancers.<sup>2</sup> We also investigated G12C as there are novel promising covalent inhibitors (AMG510 and MRTX849) that react with the cysteine sidechain and have already reached phase 3 studies.<sup>25–</sup>

29

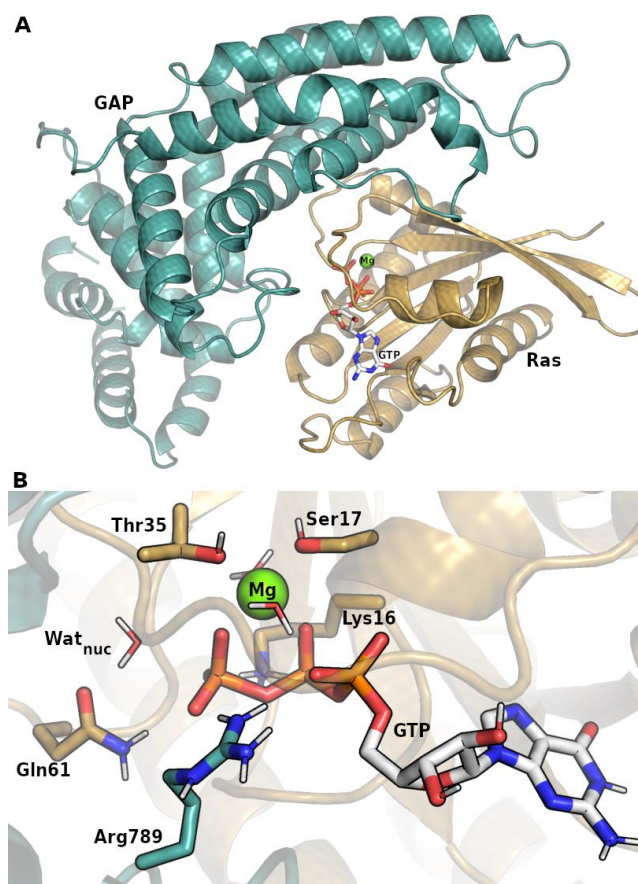


Figure 1. **A:** Ras (gold cartoon)-GAP (blue cartoon) model based on PDB ID 1WQ1. **B:** GTP (white sticks) alongside with  $Mg^{2+}$ -coordinating residues. Arginine finger (blue sticks) from p120GAP coordinates the GTP.

Experimentally, Ras structures are well characterized, and transition state (TS) analogues are available in Ras.GAP bound complexes.<sup>30</sup> We used the Ras.p120GAP complex (PDB ID 1WQ1) as the starting structure for our simulations (Supporting Information section I).<sup>31</sup>

The active site of Ras and the main associative phosphate cleavage reaction is well established (Figure 2A). An essential  $Mg^{2+}$  ion coordinates the  $\beta$ - and  $\gamma$ -phosphates,<sup>32</sup> Ser17, Thr35 of the RAS effector lobe and two water molecules.<sup>33</sup> The nucleophilic water molecule is positioned near the  $\gamma$ -phosphate via H-bonding to Gln61:O $\epsilon$  and the Gly60 backbone. The important arginine finger, Arg789 of the GAP coordinates the GTP.

The catalytic mechanism, however, still leaves many questions unanswered. The main controversy involves the proton transfer mechanism of the GTP hydrolysis reaction.<sup>34,35</sup> Upon hydrolysis, the nucleophilic water gets deprotonated while one of the oxygens of the formed inorganic (dihydrogen)phosphate (P<sub>i</sub>) gets protonated. Potential mechanisms were proposed to be (i) a direct transfer (substrate assisted or 1 water, 1W mechanism, Figure 2B), (ii) via an additional water molecule (solvent assisted or 2 water, 2W mechanism, Figure 2C), or (iii) catalyzed by a basic protein residue (general base assisted, Figure 2D).<sup>34</sup>

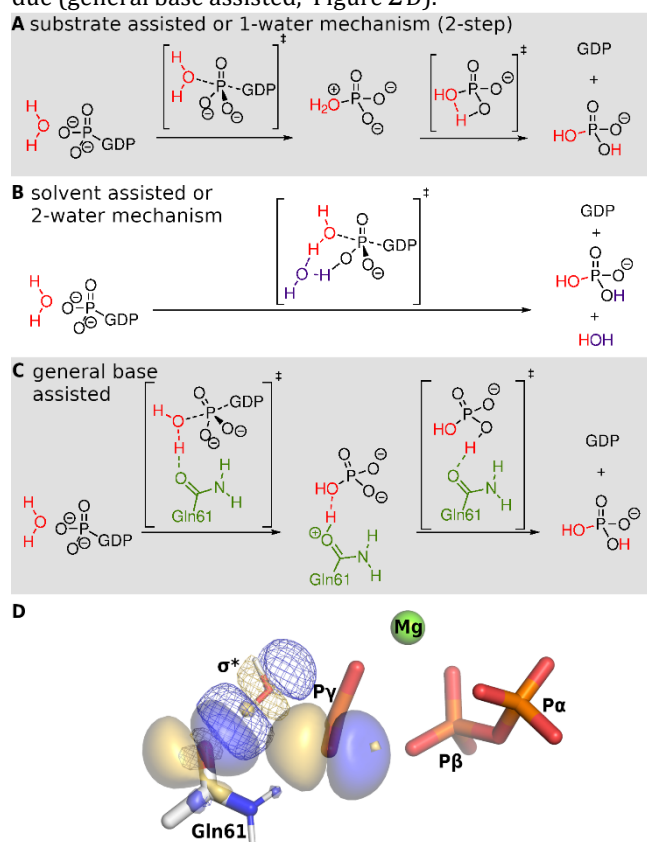


Figure 2. **A-C**: Proton transfer alternatives during GTP hydrolysis. **D**: Natural bonding orbitals during the phosphate cleavage. Solid surfaces represent occupied NBOs (lone pairs), meshes depict the virtual antibonding orbital of the  $Wat_{nuc}$  O-H bond. The electron donation from the axial direction by O $\epsilon$  of Gln61 is more favorable than the donation from the phosphate oxygen.

Despite multiple studies proposing reaction mechanisms for wild type (WT) Ras, very little is known about how detrimental changes in enzyme activity are induced by oncogenic mutations. Experimental kinetic measurements are nevertheless widely available for WT and mutant Ras proteins,<sup>12,22,36</sup> pointing to the loss of catalytic activity due to

the impaired rate of hydrolysis. Computational studies elaborated on the changes in the reactant state (RS, Figure 3A) Ras.GTP complex structures upon Gly12, and Gln61 mutations,<sup>37-43</sup> including in-depth analysis of the changes in atomic charges and the polarization of the active site before the reaction.<sup>44</sup> However, calculations to evaluate the influence of the important oncogenic changes on the reaction mechanism are missing.

To assess the structural changes caused by the key oncogenic mutations of Gly12, G12C and G12D, we analyzed classical molecular dynamics (MD) trajectories (Supporting Information section II). In general, the Cys12 substitution causes a less disruption in the active site conformations, while the Asp12 substitution induces more notable changes, such as weakening the interaction of the GTP with the Switch I loop (Table S2-3). Importantly, both mutations affect the contact with Gln61, and the interactions with the side chain are about 50% present during the simulations, while with Gly12 such interactions are absent. Given the essential role of Gln61 in the hydrolysis, this interaction is likely to contribute to the diminishing activity. The stabilizing role of Gln61 in the H-bonding pattern in the RS was previously also highlighted.<sup>45</sup> Accordingly, G12C and G12D mutations were found to induce conformational changes in Gln61.<sup>37</sup> Re-arrangements of water molecules were observed at the active site, consistently with our MD simulations. The disturbance of the water distribution was also observed in many Gln61 mutants.<sup>46</sup> Nevertheless, no major structural changes were otherwise identified in the active site. Therefore, these changes alone may not account for the major loss of activity in the Gly12 mutants.

To reveal how these key oncogenic mutations act on the catalytic pathway, we first explored the WT Ras.GAP reaction mechanism, including the proton transfer steps using QM/MM free energy calculations (Supporting Information section IV). We found that the substrate assisted transfer (1W) to the phosphate (Figure 2B) has a large barrier (Figure S2) and it is likely unfeasible due to the orbital orientation of the breaking bond. Figure 3B depicts two lone pair Natural Bonding Orbitals (NBOs) that may donate electron density towards the unoccupied O-H antibonding orbital of the  $Wat_{nuc}$  to demonstrate the significant advantage of the orientation provided by Gln61. The perturbation of the Gln61:O $\epsilon$  lone pair is two orders of magnitude higher than that of the lone pair of the O3 $\gamma$  (Table S5). We therefore included additional water molecules to facilitate this proton transfer (Figure 2C), however, these attempts also produced a high barrier (Figure S3). The importance of Gln61 was recognized by early studies,<sup>47,48</sup> by activating the  $Wat_{nuc}$ . Initially, we used constrained QM/MM minimizations to explore the mechanism to form the phosphate product by tautomerizing Gln61 into an imide, suggested by Warshel et al.<sup>49</sup> and Nemukhin et al.<sup>50</sup> Our attempts to establish an intermediate with the imide form of Gln61 failed and the N $\epsilon$  regained the proton from the phosphate.<sup>51</sup> Instead, we obtained the lowest barrier energy minimized path via a transient proton transfer to the key Gln61 residue via Gln61:O $\epsilon$  (Figure 2D). In our simulations, the rate-determining step is the protonation of the inorganic phosphate by the transient GlnH<sup>+</sup>. A similar mechanism was proposed recently by Nemukhin et al for the catalytic

mechanism of Ran GTPase,<sup>51,52</sup> and was also listed as one of the possible options for the Rho GTPase mechanism by Blackburn et al.<sup>53</sup> Previous calculations based on the PM3 semiempirical method suggested that the Gln61 is not basic enough,<sup>54</sup> which underlines the need for high level QM methodology. Gln61 was nevertheless suggested to serve as a base in very early studies,<sup>55</sup> although we find that the proton transfer is tightly coupled to the phosphate cleavage and does not take place *a priori* as a separate step.<sup>55</sup>

The five stationary points of our proposed mechanism are depicted in Figure 3. The first transitions state (TS1)

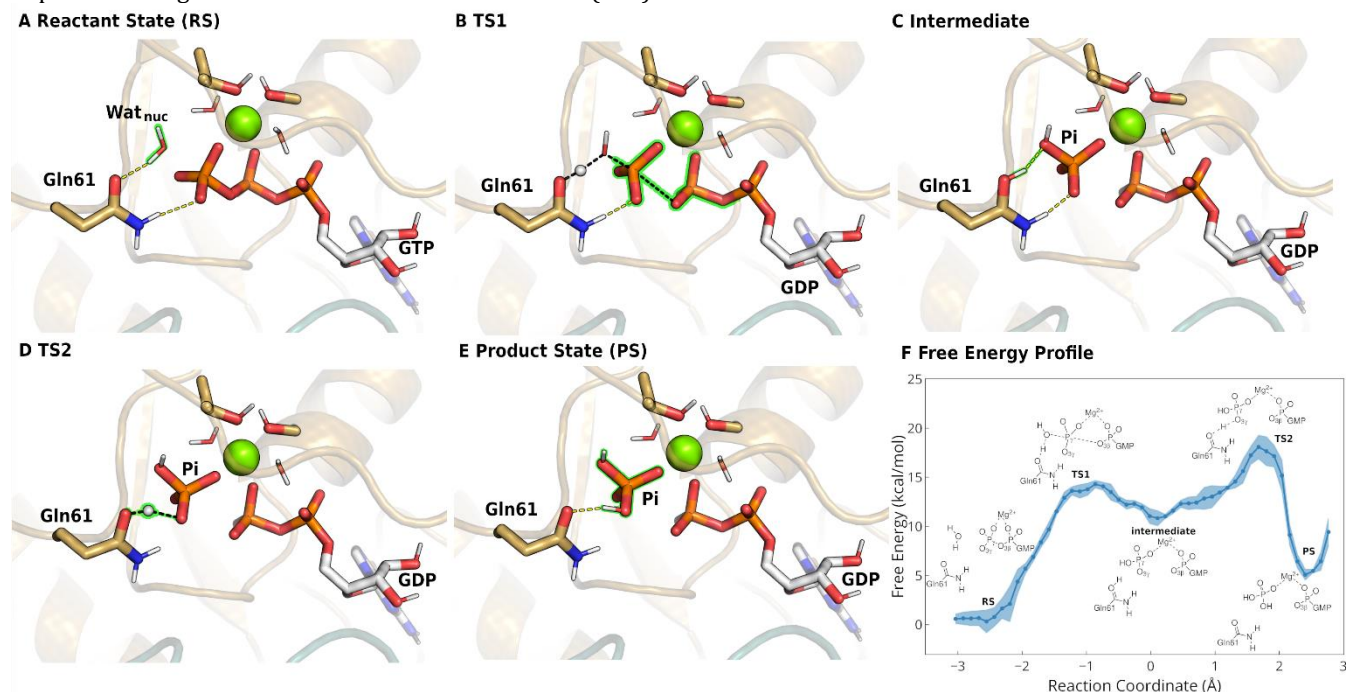


Figure 3. Stationary points along the wild type Ras.GAP GTP hydrolysis. Breaking and forming bonds (black dashes), hydrogen bonds (yellow dashes) are depicted. **A:** Reactant state. **B:** First transitions state. **C:** Intermediate with protonated Gln61. **D:** Second transition state. **E:** Product state of a bound GDP+Pi. For clarity, non-polar hydrogens are omitted. **F:** Free energy reaction profile from string calculations projected along reaction coordinate, as defined in the Supporting Information section VII. Shades depict the estimated variation of the profile along the energy axis. Stationary structures are drawn schematically.

The optimized reaction profile was used as the starting point for the finite-temperature string method (Supporting Information section VII). The free energy profile is reconstructed using WHAM<sup>56</sup> and is depicted, along with the estimated uncertainty, in **Error! Reference source not found..** The overall barrier corresponds to the second, rate-determining step is  $18.1 \pm 1.6$  kcal/mol, in good agreement with experimental rates (Table 1).

Nevertheless, despite that the current mechanism seems highly likely, we cannot exclude larger structural changes that might accompany, or prelude, the second proton transfer. This is also possible, considering available structural data, as GDP-bound Ras has a distinct switch I-II domain conformation,<sup>57</sup> and such a conformational change must take place after the cleavage of the gamma phosphate. However, the current QM/MM-based methods would not be able to capture such significant structural rearrangements, even if the timescale is fast, and future work will be needed to evaluate this mechanism.

corresponds to the nucleophilic substitution on the phosphorus and the proton transfer from Wat<sub>nuc</sub> to the Gln61 (Figure 3C). The obtained intermediate (Figure 3D), characterized by the protonated Gln61, is in strong H-bonding interaction with the newly formed inorganic phosphate. This interaction is being broken during the second, rate-limiting transition state (TS2, Figure 3E), whereby the phosphate rotates to enable the proton transfer from the O<sub>ε</sub> of the Gln61. In the direct product complex (PS, Figure 3F), the P<sub>i</sub> remains in coordination with the Mg<sup>2+</sup>.

Subsequently, using our WT mechanism as the starting point, we also investigated the reaction paths for the G12D and G12C replacements. Reaction barriers from constrained QM/MM minimizations along the path (Figure 4, orange and red, respectively) are in good agreement with experimental rates (Table 1).

**Table 1. Computational and experimental activation barriers of GTP hydrolysis catalyzed by Ras.GAP.**

	WT	G12C	G12D
calculations	<b>18.1</b>		
	22.5	24.3	27.1
	16.4 <sup>a</sup>	23.1	24.3
experiments	20.1 <sup>b</sup>	23.4	22.5
	21.4 <sup>c</sup>	-	24.4

**Bold:** free energy based on string calculations; *Italic:* potential energies obtained from constrained optimizations. Experimental barriers were calculated from rates assuming first-order kinetics. <sup>a</sup>Wey et al.<sup>58</sup> <sup>b</sup>Hunter et al.<sup>36</sup> <sup>c</sup>Johnson et al.<sup>59</sup> All energy values are in kcal/mol.



G12C presents a smaller change of 1.8 kcal/mol in the activation barrier of the Ras.GAP reaction in accordance with the smaller structural changes observed during the MD simulations. It only increases the barrier of the second step, required to complete the proton transfer to the inorganic phosphate. On the other hand, the G12D barrier is higher than the WT for both steps, increasing the barrier by 4.6 kcal/mol. Moreover, the second transition state position along the reaction coordinate is shifted towards the intermediate. This is due to the destabilization of the intermediate as the proton transfers to the Gln61 earlier than in the other cases (Figure S4). Interestingly, the proton transfer to Gln61 occurs earlier in the reaction path (Figure S4). The comparison of the NBO charges reveals that in the first reaction step the electron density (as measured by the cumulative charge) at the attacking water is slightly reduced by the G12D mutation (+0.035). This lowers its nucleophilicity and is thereby a possible explanation for the observed barrier increase. In the case of the G12C mutation, this change is significantly smaller (+0.008) and the barrier does not change compared to the WT (Table S8). This is consistent with experimental rates observed by Wey et al, whereby a larger change in the rates is observed for G12D.<sup>58</sup>

Our general base assisted mechanism is also supported by experimental findings that the Q61E mutant Ras has an increased intrinsic GTPase activity.<sup>54,60</sup> In other phosphatases, a stronger Brønsted base is often used. For example, the GTPases hGBP1<sup>61</sup> and FeoB,<sup>62</sup> as well as the ATP dependent myosin motor domain<sup>63</sup> use a glutamate as a base, accessed through a proton relay. Analogous roles for sidechain-assisted proton transfer also involves aspartate (e.g., for dUTPase<sup>64</sup>) or histidine residues (for RNase H, RNase T or RuvC)<sup>65</sup> in other phosphate cleaving enzymes. Nevertheless, the identification of the base is often a challenge for mechanistic studies.

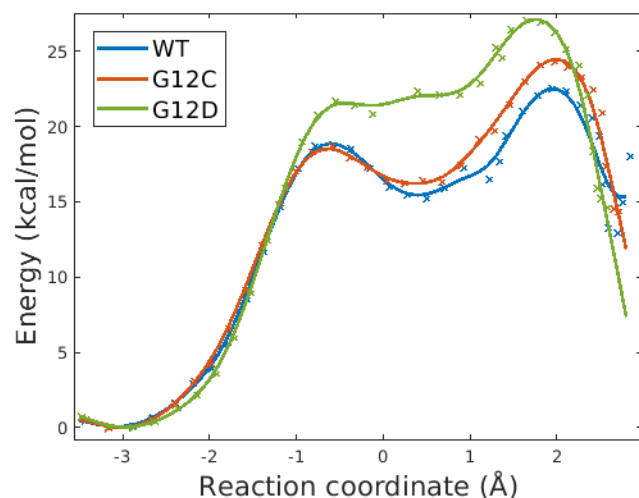


Figure 4. QM/MM energy from constrained minimizations of the WT (blue), G12C (red), and G12D (green) Ras using the reaction coordinate, as defined in the Supporting Information section VII.

In conclusion, we present a detailed mechanism for Ras.GAP catalyzed reaction using QM/MM free energy calculations. Importantly, the obtained mechanism also allows us to compare reaction rates for two key oncogenic mutations: G12C and G12D. The agreement observed with

experimental rates validates the detailed proton transfer steps that involve the crucial Gln61 residue as proton acceptor. This mechanism opens up a starting point for computational screening to develop small molecule binders that, instead of inhibiting the enzyme reaction, restore the GTPase activity of oncogenic Ras and turn aberrant signaling off.

## ASSOCIATED CONTENT

Computational details, alternative mechanism and NBO analysis (PDF)

## AUTHOR INFORMATION

### Corresponding Author

Edina Rosta – Department of Physics and Astronomy, Faculty of Maths & Physical Sciences, University College London, London WC1E 6BT, U.K. [orcid.org/0000-0002-9823-4766](https://orcid.org/0000-0002-9823-4766) Email: [e.rosta@ucl.ac.uk](mailto:e.rosta@ucl.ac.uk)

### Authors

Dénes Berta – Department of Physics and Astronomy, Faculty of Maths & Physical Sciences, University College London, London WC1E 6BT, U.K. [orcid.org/0000-0002-8299-3784](https://orcid.org/0000-0002-8299-3784)

Sascha Gehrke – Department of Physics and Astronomy, Faculty of Maths & Physical Sciences, University College London, London WC1E 6BT, U.K. [orcid.org/0000-0002-9298-6510](https://orcid.org/0000-0002-9298-6510)

### Author Contributions

All authors have given approval to the final version of the manuscript.

## ACKNOWLEDGMENT

We thank Magd Badaoui for help with the MD simulations. We also thank Beáta Vértessy and Kinga Nyíri for fruitful discussions. Authors acknowledge funding from ERC Starting Grant (Project 757850 BioNet) and EPSRC (grant no. EP/R013012/1). ER thanks funding from EPSRC (EP/R013012/1). This project made use of time on ARCHER granted via the UK High-End Computing Consortium for Biomolecular Simulation, HECBioSim (<http://hecbiosim.ac.uk>) and the CAMP HPC cluster of The Francis Crick Institute. The authors acknowledge use of the research computing facility at King's College London, Rosalind (<https://rosalind.kcl.ac.uk>).

## REFERENCES

1. Mysore, V. P. *et al.* A structural model of a Ras–Raf signalosome. *Nat Struct Mol Biol* **28**, 847–857 (2021).
2. Hobbs, G. A., Der, C. J. & Rossman, K. L. RAS isoforms and mutations in cancer at a glance. *J Cell Sci* **129**, 1287–1292 (2016).
3. Papke, B. *et al.* Silencing of Oncogenic KRAS by Mutant-Selective Small Interfering RNA. *ACS Pharmacol Transl Sci* **4**, 703–712 (2021).
4. Fan, G., Lou, L., Song, Z., Zhang, X. & Xiong, X.-F. Targeting mutated GTPase KRAS in tumor therapies. *Eur J Med Chem* **226**, 113816 (2021).
5. Aran, V. *et al.* Identification of mutant K-RAS in pituitary macroadenoma. *Pituitary* **24**, 746–753 (2021).

6. Bilal, F. *et al.* The Transcription Factor SLUG Uncouples Pancreatic Cancer Progression from the RAF–MEK1/2–ERK1/2 Pathway. *Cancer Res* **81**, 3849–3861 (2021).
7. Phipps, A. I. *et al.* KRAS-mutation status in relation to colorectal cancer survival: the joint impact of correlated tumour markers. *Br J Cancer* **108**, 1757–1764 (2013).
8. Teo, M. Y. M., Fong, J. Y., Lim, W. M. & In, L. L. A. Current Advances and Trends in KRAS Targeted Therapies for Colorectal Cancer. *Molecular Cancer Research* **20**, 30–44 (2022).
9. Burd, C. E. *et al.* Mutation-Specific RAS Oncogenicity Explains NRAS Codon 61 Selection in Melanoma. *Cancer Discov* **4**, 1418–1429 (2014).
10. Fedorenko, I. v, Gibney, G. T., Sondak, V. K. & Smalley, K. S. M. Beyond BRAF: where next for melanoma therapy? *Br J Cancer* **112**, 217–226 (2015).
11. Randic, T., Kozar, I., Margue, C., Utikal, J. & Kreis, S. NRAS mutant melanoma: Towards better therapies. *Cancer Treat Rev* **99**, 102238 (2021).
12. Xie, C. *et al.* Identification of a New Potent Inhibitor Targeting KRAS in Non-small Cell Lung Cancer Cells. *Front Pharmacol* **8**, (2017).
13. Nacarino-Palma, A. *et al.* Loss of Aryl Hydrocarbon Receptor Favors K-RasG12D-Driven Non-Small Cell Lung Cancer. *Cancers (Basel)* **13**, 4071 (2021).
14. Jakob, J. A. *et al.* NRAS mutation status is an independent prognostic factor in metastatic melanoma. *Cancer* **118**, 4014–4023 (2012).
15. Abe, J. *et al.* Novel activating KRAS mutation candidates in lung adenocarcinoma. *Biochem Biophys Res Commun* **522**, 690–696 (2020).
16. Jácome, A. A. *et al.* The prognostic impact of RAS on overall survival following liver resection in early versus late-onset colorectal cancer patients. *Br J Cancer* **124**, 797–804 (2021).
17. Cox, A. D., Fesik, S. W., Kimmelman, A. C., Luo, J. & Der, C. J. Drugging the undruggable RAS: Mission Possible? *Nat Rev Drug Discov* **13**, 828–851 (2014).
18. Rudack, T. *et al.* The Ras dimer structure. *Chem Sci* **12**, 8178–8189 (2021).
19. Molina-Arcas, M., Samani, A. & Downward, J. Drugging the Undruggable: Advances on RAS Targeting in Cancer. *Genes (Basel)* **12**, 899 (2021).
20. Lyons, J. *et al.* Two G Protein Oncogenes in Human Endocrine Tumors. *Science (1979)* **249**, 655–659 (1990).
21. Lu, S., Jang, H., Gu, S., Zhang, J. & Nussinov, R. Drugging Ras GTPase: a comprehensive mechanistic and signaling structural view. *Chem Soc Rev* **45**, 4929–4952 (2016).
22. Gideon, P. *et al.* Mutational and kinetic analyses of the GTPase-activating protein (GAP)-p21 interaction: the C-terminal domain of GAP is not sufficient for full activity. *Mol Cell Biol* **12**, 2050–2056 (1992).
23. Mishra, A. K. & Lambright, D. G. Small GTPases and their GAPs. *Biopolymers* **105**, 431–448 (2016).
24. Nagy, G. N. *et al.* Structural Characterization of Arginine Fingers: Identification of an Arginine Finger for the Pyrophosphatase dUTPases. *J Am Chem Soc* **138**, 15035–15045 (2016).
25. Ostrem, J. M., Peters, U., Sos, M. L., Wells, J. A. & Shokat, K. M. K-Ras(G12C) inhibitors allosterically control GTP affinity and effector interactions. *Nature* **503**, 548–551 (2013).
26. Patricelli, M. P. *et al.* Selective Inhibition of Oncogenic KRAS Output with Small Molecules Targeting the Inactive State. *Cancer Discov* **6**, 316–329 (2016).
27. Lindsay, C. R. & Blackhall, F. H. Direct Ras G12C inhibitors: crossing the rubicon. *Br J Cancer* **121**, 197–198 (2019).
28. Kwan, A. K., Piazza, G. A., Keeton, A. B. & Leite, C. A. The path to the clinic: a comprehensive review on direct KRASG12C inhibitors. *Journal of Experimental & Clinical Cancer Research* **41**, 27 (2022).
29. Canon, J. *et al.* The clinical KRAS(G12C) inhibitor AMG 510 drives anti-tumour immunity. *Nature* **575**, 217–223 (2019).
30. Gasper, R. & Wittinghofer, F. The Ras switch in structural and historical perspective. *Biol Chem* **401**, 143–163 (2019).
31. Scheffzek, K. *et al.* The Ras-RasGAP Complex: Structural Basis for GTPase Activation and Its Loss in Oncogenic Ras Mutants. *Science (1979)* **277**, 333–339 (1997).
32. Mann, D., Güldenhaupt, J., Schartner, J., Gerwert, K. & Köttig, C. The protonation states of GTP and GppNHp in Ras proteins. *Journal of Biological Chemistry* **293**, 3871–3879 (2018).
33. Rudack, T. *et al.* Catalysis of GTP Hydrolysis by Small GTPases at Atomic Detail by Integration of X-ray Crystallography, Experimental, and Theoretical IR Spectroscopy. *Journal of Biological Chemistry* **290**, 24079–24090 (2015).
34. Berta, D., Buigues, P. J., Badaoui, M. & Rosta, E. Cations in motion: QM/MM studies of the dynamic and electrostatic roles of H<sup>+</sup> and Mg<sup>2+</sup> ions in enzyme reactions. *Curr Opin Struct Biol* **61**, 198–206 (2020).
35. Carvalho, A. T. P., Szeler, K., Vavitsas, K., Åqvist, J. & Kamerlin, S. C. L. Modeling the mechanisms of biological GTP hydrolysis. *Arch Biochem Biophys* **582**, 80–90 (2015).
36. Hunter, J. C. *et al.* Biochemical and Structural Analysis of Common Cancer-Associated KRAS Mutations. *Molecular Cancer Research* **13**, 1325–1335 (2015).

37. Menyhárd, D. K. *et al.* Structural impact of GTP binding on downstream KRAS signaling. *Chem Sci* **11**, 9272–9289 (2020).
38. Chen, J., Zeng, Q., Wang, W., Hu, Q. & Bao, H. Q61 mutant-mediated dynamics changes of the GTP-KRAS complex probed by Gaussian accelerated molecular dynamics and free energy landscapes. *RSC Adv* **12**, 1742–1757 (2022).
39. Sharma, N., Sonavane, U. & Joshi, R. Comparative MD simulations and advanced analytics based studies on wild-type and hot-spot mutant A59G HRas. *PLoS One* **15**, e0234836 (2020).
40. Wang, X. Conformational Fluctuations in GTP-Bound K-Ras: A Metadynamics Perspective with Harmonic Linear Discriminant Analysis. *J Chem Inf Model* **61**, 5212–5222 (2021).
41. Vatansever, S., Erman, B. & Gümüş, Z. H. Comparative effects of oncogenic mutations G12C, G12V, G13D, and Q61H on local conformations and dynamics of K-Ras. *Comput Struct Biotechnol J* **18**, 1000–1011 (2020).
42. Pantsar, T. *et al.* Assessment of mutation probabilities of KRAS G12 missense mutants and their long-timescale dynamics by atomistic molecular simulations and Markov state modeling. *PLoS Comput Biol* **14**, e1006458 (2018).
43. Khrenova, M. G., Mironov, V. A., Grigorenko, B. L. & Nemukhin, A. v. Modeling the Role of G12V and G13V Ras Mutations in the Ras-GAP-Catalyzed Hydrolysis Reaction of Guanosine Triphosphate. *Biochemistry* **53**, 7093–7099 (2014).
44. Tichauer, R. H., Favre, G., Cabantous, S. & Brut, M. Hybrid QM/MM vs Pure MM Molecular Dynamics for Evaluating Water Distribution within p21 N-ras and the Resulting GTP Electronic Density. *J Phys Chem B* **123**, 3935–3944 (2019).
45. Zeng, J. *et al.* Conformational Features of Ras: Key Hydrogen-Bonding Interactions of Gln61 in the Intermediate State during GTP Hydrolysis. *J Phys Chem B* **125**, 8805–8813 (2021).
46. Tichauer, R. H. *et al.* Water Distribution within Wild-Type NRas Protein and Q61 Mutants during Unrestrained QM/MM Dynamics. *Biophys J* **115**, 1417–1430 (2018).
47. Krengel, U. *et al.* Three-dimensional structures of H-ras p21 mutants: Molecular basis for their inability to function as signal switch molecules. *Cell* **62**, 539–548 (1990).
48. Pai, E. F. *et al.* Refined crystal structure of the triphosphate conformation of H-ras p21 at 1.35 Å resolution: implications for the mechanism of GTP hydrolysis. *EMBO J* **9**, 2351–2359 (1990).
49. B, R. P., Plotnikov, N. v., Lameira, J. & Warshel, A. Quantitative exploration of the molecular origin of the activation of GTPase. *Proceedings of the National Academy of Sciences* **110**, 20509–20514 (2013).
50. Mironov, V. A., Khrenova, M. G., Lychko, L. A. & Nemukhin, A. v. Computational characterization of the chemical step in the GTP hydrolysis by Ras-GAP for the wild-type and G13V mutated Ras. *Proteins: Structure, Function, and Bioinformatics* **83**, 1046–1053 (2015).
51. Khrenova, M. G., Grigorenko, B. L. & Nemukhin, A. v. Molecular Modeling Reveals the Mechanism of Ran-Ran-GAP-Catalyzed Guanosine Triphosphate Hydrolysis without an Arginine Finger. *ACS Catal* **11**, 8985–8998 (2021).
52. Molt, R. W., Pellegrini, E. & Jin, Y. A GAP-GTPase-GDP-P<sub>i</sub> Intermediate Crystal Structure Analyzed by DFT Shows GTP Hydrolysis Involves Serial Proton Transfers. *Chemistry – A European Journal* **25**, 8484–8488 (2019).
53. Jin, Y., Molt, R. W., Waltho, J. P., Richards, N. G. J. & Blackburn, G. M. 19 F NMR and DFT Analysis Reveal Structural and Electronic Transition State Features for RhoA-Catalyzed GTP Hydrolysis. *Angewandte Chemie* **128**, 3379–3383 (2016).
54. Martín-García, F., Mendieta-Moreno, J. I., López-Viñas, E., Gómez-Puertas, P. & Mendieta, J. The Role of Gln61 in HRas GTP Hydrolysis: A Quantum Mechanics/Molecular Mechanics Study. *Biophys J* **102**, 152–157 (2012).
55. Langen, R., Schweins, T. & Warshel, A. On the mechanism of guanosine triphosphate hydrolysis in ras p21 proteins. *Biochemistry* **31**, 8691–8696 (1992).
56. Kumar, S., Rosenberg, J. M., Bouzida, D., Swendsen, R. H. & Kollman, P. A. The weighted histogram analysis method for free-energy calculations on biomolecules. I. The method. *J Comput Chem* **13**, 1011–1021 (1992).
57. Kolch, W., Berta, D. & Rosta, E. Dynamic Regulation of RAS and RAS Signaling. *Biochemical Journal* (2022).
58. Wey, M., Lee, J., Jeong, S. S., Kim, J. & Heo, J. Kinetic Mechanisms of Mutation-Dependent Harvey Ras Activation and Their Relevance for the Development of Costello Syndrome. *Biochemistry* **52**, 8465–8479 (2013).
59. Johnson, C. W. *et al.* Regulation of GTPase function by autophosphorylation. *Mol Cell* **82**, 950–968.e14 (2022).
60. Frech, M. *et al.* Role of Glutamine-61 in the Hydrolysis of GTP by p21H-ras: An Experimental and Theoretical Study. *Biochemistry* **33**, 3237–3244 (1994).
61. Tripathi, R., Noetzel, J. & Marx, D. Exposing catalytic versatility of GTPases: taking reaction detours in mutants of hGBP1 enzyme without additional energetic cost. *Physical Chemistry Chemical Physics* **21**, 859–867 (2019).
62. Vithani, N., Batra, S., Prakash, B. & Nair, N. N. Elucidating the GTP Hydrolysis Mechanism in FeoB: A Hydrophobic Amino-Acid Substituted GTPase. *ACS Catal* **7**, 902–906 (2017).
63. Lu, X., Ovchinnikov, V., Demapan, D., Roston, D. & Cui, Q. Regulation and Plasticity of Catalysis in Enzymes: Insights from Analysis of Mechanochemical Coupling in Myosin. *Biochemistry* **56**, 1482–1497 (2017).

64. Lopata, A. *et al.* Mutations Decouple Proton Transfer from Phosphate Cleavage in the dUTPase Catalytic Reaction. *ACS Catal* **5**, 3225–3237 (2015).
65. Dürr, S. L. *et al.* The Role of Conserved Residues in the DEDDh Motif: the Proton-Transfer Mechanism of HIV-1 RNase H. *ACS Catal* **11**, 7915–7927 (2021).

